Jour. of the KGS, Vol. 20, No. 7. September 2004, pp. 25~32

Case History Evaluation of Axial Behavior of Micropiles

소구경말뚝의 축방향 거동에 대한 사례 연구

Jeon, Sang-Soo[1] 전 상 수

요 지

본 논문은 소구경말뚝의 현장시험결과를 조사하고 축방향 변위와 흙의 성질과의 상관관계에 따른 말뚝의 주변마찰력을 산정하기 위하여 종합적으로 검토하였다. 점착력과 비점착력의 성질을 가진 흙에 대하여 조사를 하였다. 현장적용 목적에 부합한 소구경말뚝의 하중-변위관계와 지반공학적 흙의 특성 그리고 흙의 종류에 대한 연구가 정규화평균값과 경험관계식을 통하여 이루어졌다. 대구경말뚝과 압력-그라우팅 설치 효과로 인한 소구경말뚝의 하중전이로 인한 지지력은 현저한 차이가 있었다. 특히 말뚝 근입깊이(D)와 말뚝 직경(B)의 비가 100보다 작은 얕은 깊이에서는 소구경말뚝이 대구경말뚝에 비해 현저하게 뛰어난 지지력을 가지고 있음을 알 수 있었으며 점착력이 있는 흙에서는 약 1.5에서 최고 2.5배정도 비점착력인 흙에서는 약 1.5에서 2.5배 그리고 최고 6배의 지지력을 갖고 있음을 알 수 있다.

Abstract

This paper examines the results of full-scale field tests on micropiles and side resistance is evaluated with respect to axial displacements and soil properties. Both cohesive and cohesionless soils are included in this evaluation. For all practical purposes, the developed load-displacement relationship and the geotechnical soil properties for each micropile and soil type can be used to represent the available data well through normalized average values and empirical correlations. There is a significant difference in load-carrying capacity between micropiles and drilled shafts that results primarily from the micropile pressure-grouting installation effects on the state of stress in the ground. The results show that micropiles can have a significant increase of capacity over larger-diameter drilled shafts at shallower depths with D/B < 100 or so. In cohesive soils, the typical increase is on the order of 1.5 with values as high as 2.5. For cohesionless soils, the typical increases are in the range of 1.5 to 2.5 with values as high as 6.

Keywords : Axial behavior, Empirical correlations, Full-scale field test, Micropiles, Soil properties

1. Introduction

Micropiles have a high ratio of the circumference to the cross-section area, and therefore their load capacity rely essentially on side resistance considering the load transfer mechanism. Tip resistance may be negligible in most cases. Micropiles have been used widely for foundations, under-pinning, slide stabilization, etc. Their development generally is attributed to the pioneering work of Lizzi in Italy during the 1950s (Lizzi, 1982).

Specific analysis and design methodologies for micropiles are limited and largely empirical. Often, empirical rules and procedures developed for larger-diameter drilled shafts have been used for micropile design. However, micropile load tests have shown that this approach generally results in conservative designs.

In this paper, the behavior of micropiles is examined in both cohesive and cohesionless soils under axial

1 Member, Chief Researcher, Korea Highway & Transportation Technology, Korea Highway Corporation (ssj3@freeway.co.kr)

compression loading. Case histories are examined, and a detailed evaluation is made of the load test results, focusing primarily on the prediction of side resistance and the load-displacement response using conventional geotechnical parameters and analyses (Jeon, 2004).

2. Classification of Micropiles and Database

Micropiles often are classified into Types A-D, primarily on the basis of grouting type and pressure (e.g., Bruce and Juran, 1997). Type A is where the cement grout is placed under gravity head only, much like a drilled shaft. In Type B, neat cement grout is injected into the drilled hole as the temporary drill casing is withdrawn. Grout pressures typically are in the range of 0.3 to 1 MN/m^2 and are limited by the need to maintain a tight grout "seal" around the casing and to avoid hydrofracturing and/or excessive grout consumptions. Types C and D employ initial gravity placement of grout followed by secondary "global" pressure grouting in single (C) or multiple applications (D). Type C is common only in France.

The database developed for this study included the case histories from three sites with eight field load tests conducted in cohesive soils and from seven sites with thirteen field load tests conducted in cohesionless soils. The site, micropile, and geotechnical data for each load test are summarized in Table 1. These data are obtained from published and unpublished sources, which are indicated in the table footnotes. There are two sites located in the United Kingdom, one in Hong Kong, one in Germany, one in Japan, and five in the United States. In all cases, general descriptions of the soil profiles for cohesionless soils and the undrained shear strength for cohesive soils are reported. However, in most of the case histories, further details are not given. Since the actual soil properties are limited, the average values of effective stress friction angle and overconsolidation ratio (OCR) were estimated to obtain the design soil parameters, as described later. The micropile types are B and probably D, although the references did not contain details on whether the latter were C or D.

3. Axial Behavior of Load Tests

3.1 Initial Linear Behavior of Loading Response

The initial load-displacement behavior of micropiles is influenced by several factors such as the elastic modulus of soil surrounding them, the cross sectional area of them, and the relative soil-pile interface shear displacement, which is controlled by the interface properties, the initial state of stress in the ground, and the changes that occur with pile installation and time. The elastic slope stands for the elastic pile response if it is assumed to be a free-standing column with a Young's modulus of composite pile (E), pile depth (D), and cross-sectional area (A). The elastic slope (ES) of the composite tubular cased reinforced micropile is EA/D. Especially for micropile type B, the displacement response of a micropile transferring the applied compression load P to a competent bearing stratum is assumed to correspond to the elastic shortening Δ of its portion in the unbonded weak/soil layers overlying the competent stratum.

The initial slope (IS_H) computed from the hyperbolic model is derived. The ratios of the elastic slope (ES) to each of the initial slope (IS_H) for cohesive and cohesionless soils are calculated, and the results are plotted in Figs. 1 and 2, respectively. As shown in the figure, D_b and B_s indicate the base depth and the shaft diameter of micropile, respectively. The mean and standard deviation of slope ratio (ES/IS_H) in cohesive soils are 0.30 and 0.11. Those in cohesionless soils are 0.37 and 0.25, respectively. The results indicate that the slope ratio does not exceed 1 in high depth ratio (D_b/B_s), indicating the initial linear load-displacement behavior is close to elastic. Therefore, the initial slope can be estimated by the elastic slope for micropiles subjected to axial compression loading. However, since the data is too limited, further investigations based on more sufficient data may be required.

3.2 Interpretation of Load Test Results

The "failure load"is difficult to determine, and there have been dozens of methods proposed to evaluate this

Table 1. Site and geotechnical information

Case[a]	Test Site	Soil Description	GWT[b] (m)	Shaft Diameter B (m)	Shaft Depth D (m)	Load Carrying Length (m)	Pile Type	Soil Parameter				
								L_{ST} (kN)	γ_t[c] (kN/m^3)	$\bar{\Phi}_{tc}$[d] (deg)	K_o[e]	s_u[f] (kN/m^2)
1-1	Westbourne, UK	London Clay (Silty Clay)	–	0.15	9.0	9.0	C or D	329	19.4	–	–	119
1-2	Westbourne, UK	London Clay (Silty Clay)	–	0.15	9.0	9.0	C or D	463	19.4	–	–	119
1-3	Westbourne, UK	London Clay (Silty Clay)	–	0.15	12.0	12.0	C or D	454	19.4	–	–	138
1-4	Westbourne, UK	London Clay (Silty Clay)	–	0.15	19.0	19.0	C or D	338	19.4	–	–	158
1-5	Westbourne, UK	London Clay (Silty Clay)	–	0.15	19.0	19.0	C or D	463	19.4	–	–	158
1-6	Westbourne, UK	London Clay (Silty Clay)	–	0.17	19.0	19.0	C or D	423	19.4	–	–	158
2	Herney Bay, UK	London Clay (Silty Clay)	–	0.15	13.5	13.5	C or D	356	19.4	–	–	97
3	Shatin, Hong Kong	Marine Deposits	–	0.15	30.0	30.0	C or D	601	20.9	–	–	166
4-1	Germany	Fill, Sand and Gravel	3.9	0.18	8.0	8.0	C or D	578	17.9	30.8	1.18	–
4-2	Germany	Fill, Sand and Gravel	3.9	0.18	10.0	10.0	C or D	476	18.2	32.4	1.30	–
4-3	Germany	Fill, Sand and Gravel	4.7	0.15	16.0	5.0	C or D	979	19.2	38.5	1.73	–
5-1	Augusta, GA	Clay, Dense and Sand	g	0.18	10.9	3.3	B	667	19.1	41.5	2.03	–
5-2	Augusta, GA	Clay, Dense and Sand	g	0.18	10.9	3.3	C or D	730	19.1	41.5	2.03	–
6	Boston, MA	Medium to Dense Sand	h	0.14	6.1	4.6	B	667	17.3	35.0	1.25	–
7-1	Coney Island, NY	Fine to Medium Sand	1.2	0.17	10.7	3.0	B	463	17.3	33.0	1.15	–
7-2	Coney Island, NY	Fine to Medium Sand	1.2	0.17	10.7	3.0	B	231	17.3	33.0	1.15	–
7-3	Coney Island, NY	Fine to Medium Sand	1.2	0.19	13.7	6.1	B	472	17.3	33.0	1.15	–
8	Mobile, AL	Ednse Sand and Gravel	10.0	0.18	25.0	9.4	B	961	19.2	41.5	2.03	–
9	McLean, VA	Loose to Dense Sand	9.1	0.15	11.4	7.0	B	502	18.8	35.0	1.25	–
10-1	Japan	Fine and Silty Sand	h	0.18	21.8	5.2	B	1245	18.8	35.0	1.25	–
10-2	Japan	Fine and Silty Sand	h	0.18	17.6	1.1	B	658	18.8	35.0	1.25	–

a – Sources: Case 1: Jones & Turner (1980); Case 2: Bruce, et al. (1985); Case 3: Bruce & Yeung (1984); Case 4: Koreck (1978); Case 5: Bruce (1990); Case 6: Bruce (1988); Case 7: Bruce (1987, 1988); Case 8: Bruce, et al. (1992); Case 9: Singh & Heine (1984); Case 10: Ichimura & Oshita (2000)

b – GWT = ground water table

c – γ_t = total unit weight of soil (estimated)

d – $\bar{\Phi}_{tc}$ = effective stress friction angle in triaxial compression (estimated)

e – K_o = coefficient of horizontal soil stress (estimated)

f – s_u = undrained shear strength

g – water table is below the pile tip

h – water table is not reported; assumed to be 1m from the ground surface

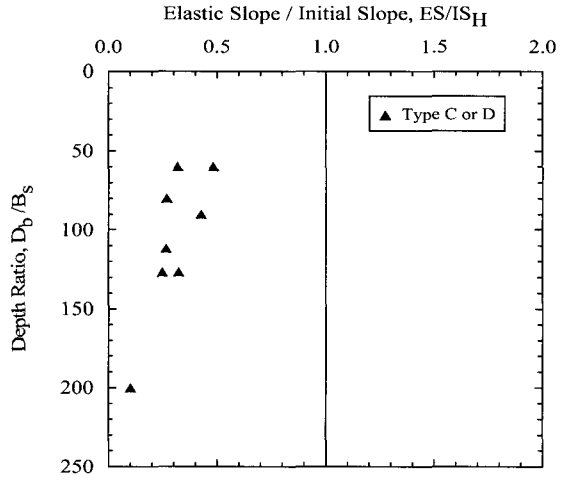

Fig. 1. Effect of foundation diameter on initial slope-displacement curve in cohesive soils for micropiles in compression

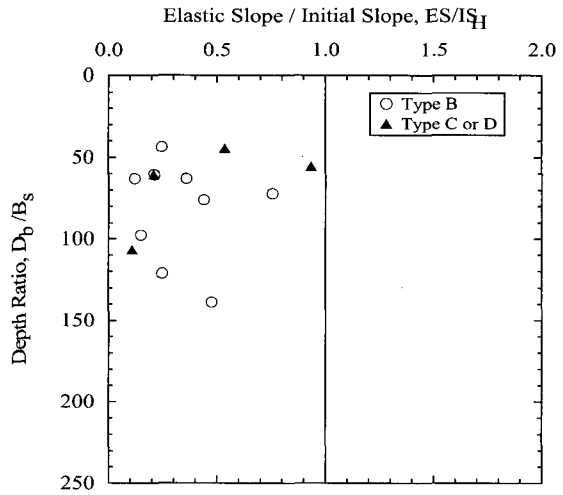

Fig. 2. Effect of foundation diameter on initial slope-displacement curve in cohesionless for micropiles in compression

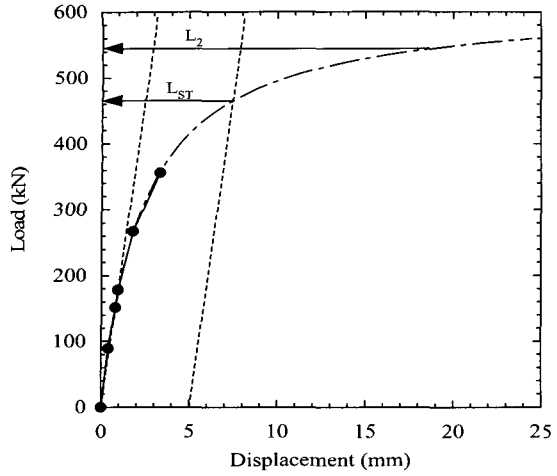

Fig. 3. Illustration of modification and extrapolation of original load versus displacement curve

value. However, Hirany and Kulhawy (1988, 1989) have shown that, from observation of load-displacement curves for drilled foundations, it is reasonable to interpret the "failure load" at L_2, which is the failure threshold that follows the nonlinear load-displacement response, at which point essentially linear response occurs. This point is illustrated in Fig. 3. Unfortunately, most of the test data did not contain sufficient data to use the L_2 method directly. Alternatively, the slope tangent method could be used for interpretation (Davisson, 1972). The slope tangent value (L_{ST}) falls in the nonlinear region below L_2, which really is too low to consider as "failure". However, this method is convenient because most test data can be interpreted using it.

Since most of the load tests are terminated before achieving true geotechnical capacity, it is not possible to interpret the failure threshold (L_2) directly from the test results. Alternatively, it has been shown that, on average, there is a consistent relationship between L_{ST} and L_2 for drilled shafts (Hirany and Kulhawy, 1988), augered cast-in-place piles (Chen, 1998), and pressure-injected footings (Chen, 1998). These studies showed that LST is approximately 0.85 L_2, so therefore L_2 can be estimated at 1.18 L_{ST} for the analyses discussed herein.

3.3 Load-Displacement Behavior

The load-displacement curves can be modeled well by the hyperbolic curve below:

$$P = \frac{\Delta}{a + m\Delta} \quad (1)$$

in which P = applied load, Δ= butt displacement, and both a and m = curve fitting parameters. This hyperbolic curve is very close to the actual load test data points, as shown in Fig. 3 for Case 1-2.

After establishing the hyperbolic curve, a straight line elastic slope is drawn through the initial points of the load-displacement curve, and a second line is drawn parallel to the first at an offset equal to 0.15 inch + B (inch)/120 (Davisson, 1972). The load corresponding to the intersection of the load-displacement curve and this offset line is the slope tangent load (L_{ST}). These procedures are applied to the twenty-one load tests reported in Table 1, and the L_2 values are given by 1.18 L_{ST}.

The twenty-one load-displacement curves are normalized by dividing the applied load by L_{ST}. These results are given in Fig. 4, which shows the normalized load versus the normalized displacement, in which the mean is plotted as well as plus and minus one standard deviation of the normalized load. To incorporate shaft diameter effects, the normalized applied load is plotted against the normalized displacement. As can be seen, the slope tangent load (L_{ST}), on average, corresponds to a displacement of approximately 5.5% and 6.5% of the shaft diameter for cohesive and cohesionless soils, respectively. Also, the average load-displacement curves

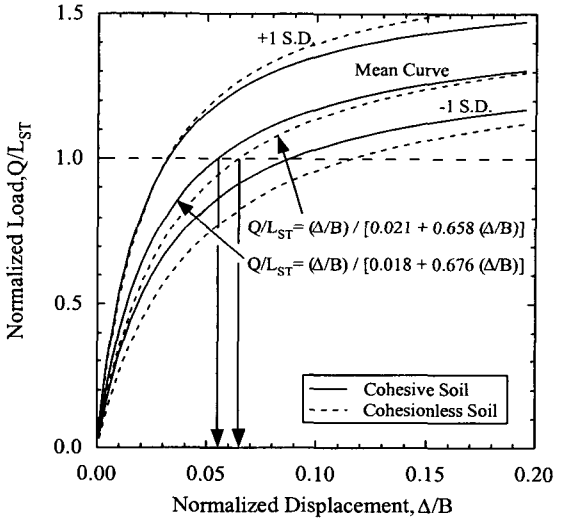

Fig. 4. Normalized load - displacement in cohesive and cohesionless soils

are very similar for both soil groupings.

4. Side Resistance in Cohesive and Cohesionless Soils

4.1 Geotechnical Analysis Parameters

The values of the geotechnical parameters are necessary for each site in the load test database to evaluate the micropile behavior. In general, the required parameters are the undrained shear strength (s_u) for cohesive soils and the effective stress friction angle ($\bar{\phi}$), overconsolidation ratio (OCR), and in-situ coefficient of horizontal soil stress (Ko) for cohesionless soils. Some of the case histories had the necessary parameters (cohesive soils), but many lacked these geotechnical parameters (cohesionless soils). Therefore, it is necessary to use theoretical and empirical correlations between the necessary parameters and those that are available, as described below (Kulhawy and Mayne, 1990).

4.2 Side Resistance in Cohesive Soils by Alpha Method

The undrained side resistance in cohesive soils commonly is evaluated by the method, which is given as (e.g., Kulhawy, 1991):

$$Q_s = \pi B \alpha \int_0^D s_u(z)\,dz \qquad (2)$$

in which α = empirical correlation factor, B = shaft diameter, D = shaft depth, s_u = undrained shear strength, and z = depth. The axial compression capacity is given by the L_2 method, and the value of α is back-calculated from the load test results as follows:

$$\alpha = \frac{Q_s(L_2)}{\pi B D s_u} \qquad (3)$$

in which $Q_s(L_2)$ = interpreted side resistance using the L_2 method, and s_u = mean undrained shear strength over depth D.

The side resistance also can be predicted from Eq. 2 using available correlations. For example, Chen and Kulhawy (1994) developed an CIUC (consolidated-isotropically undrained triaxial compression) for drilled shafts that links specifically to the soil undrained shear strength determined by CIUC triaxial tests. However, it must be remembered that the factor is a lumped constant that relies on many factors, such as construction technique, drilling disturbance on the soil, roughness of the soil-concrete interface, pore water pressure changes during loading, geotechnical soil properties, and method used to assess s_u. Fig. 5 shows the back-calculated field average unit side resistance versus depth ratio, as well as the values computed using CIUC for drilled shafts.

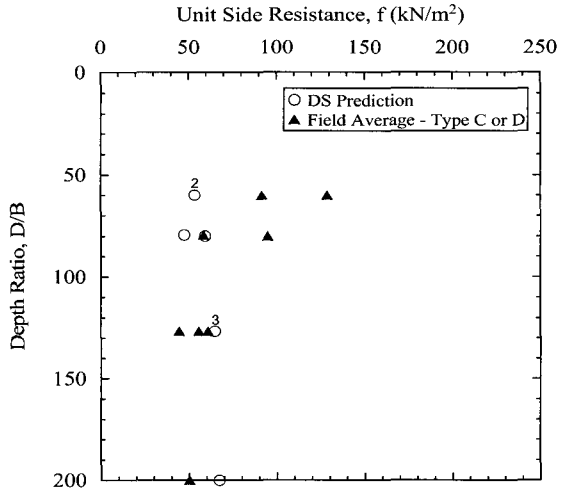

Fig. 5. Comparison of unit side resistance in cohesive soils predicted by drilled shaft (DS) calculations and back-calculated field averages

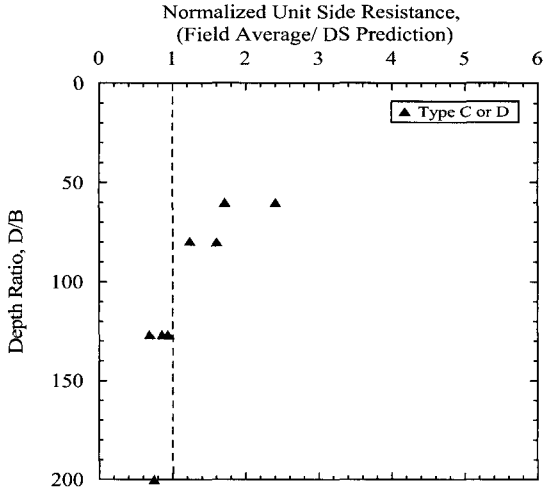

Fig. 6. Normalized unit side resistance in cohesive soils vs. depth ratio

The subscipts on the symbols refer to the number of overlapping tests. Fig. 6 shows the normalized unit side resistance versus depth ratio. These figures show that, for D/B > 100, micropiles and drilled shafts are essentially the same. However, at shallower depths, there is an apparent increase for micropiles over larger-diameter drilled shafts, by a typical factor on the order of 1.5 with values as high as 2.5. This increase results from the grouting during installation.

4.3 Side Resistance in Cohesionless Soils by Beta Method

The side resistance evaluated by the beta method is given by the interface friction of the soil-pile interface over the entire shaft depth. To account for the variation of the soil properties with depth, the soil profile was divided into different soil layers. The average geo-technical parameters are estimated at the mid-depth of each layer, assuming the effective stress friction angle and overconsolidation ratio (OCR) based on the general description of soil consistency.

The drained side resistance is given by the beta method as (e.g., Kulhawy, 1991):

$$\begin{aligned} Q_s(\beta) &= \pi B(K/K_0)\int_0^D \bar{\sigma}(z)\tan[\bar{\phi}\cdot\delta/\bar{\phi}]dz \\ &= \pi B\int_0^D \beta\,\bar{\sigma}_v(z)\,dz \\ &= \pi B\int_0^D f(z)dz \end{aligned} \quad (4)$$

in which K/K_o = factor that represents the change in the in-situ stress by construction method, $\delta/\bar{\phi}$ = interface roughness factor (= 1 for a rough soil-concrete interface), $\bar{\sigma}_v$= vertical effective stress, $\beta = K\tan\delta$, and f(z) = unit side resistance. Since the case histories did not report the effective stress friction angle and OCR, the typical values in Table 2 for effective stress friction angle and OCR as a function of soil consistency are used to calculate K_o, as given below (Kulhawy and Mayne, 1990):

$$K_0 = (1-\sin\bar{\phi}_{tc})\,OCR^{\sin\bar{\phi}_{tc}} \quad (5)$$

The K/K_o value has not been calibrated for micropiles, so a value of 1.0 that is based on good quality construction for drilled shafts is used for a first-order estimation.

The field average beta (β_m) can be computed from the following:

$$\beta_m = \frac{Q_s(L_2)}{\pi B D\,\bar{\sigma}_{vm}} \quad (6)$$

in which $Q_s(L_2)$ = interpreted side resistance from the L_2 method and $\bar{\sigma}_{vm}$= mean vertical effective stress. As the depth ratio increases, β may decrease and approach the normally consolidated (NC) range, given by:

$$\beta_{NC} = K_0\tan\delta \approx (1-\sin\bar{\phi})\tan\bar{\phi} \quad (7)$$

assuming $K/K_o = 1$ and $\delta/\bar{\phi} = 1$.

The predicted beta (β_p) can be computed from the following:

$$\beta_p = K_0(K/K_0)\tan[\bar{\phi}\cdot\delta/\bar{\phi}] \quad (8)$$

To evaluate β_p, the soil profile along the shaft depth is divided into different soil layers, and the average K_o and $\bar{\phi}$ values are estimated at mid-depth of each layer to calculate β for that layer. The value of $\delta/\bar{\phi}$ for cast-in-place shafts is taken as 1.0. Since the value of K/K_o depends on the construction method, local variations in K_o, cementation, and soil characteristics, it is very difficult to define a unique relationship for β versus depth ratio. Fig. 7 shows the back-calculated field average unit side resistance versus depth ratio, along with the predicted values assuming $K/K_o = 1$ (for drilled shafts) and the lower and upper bound of unit side resistance computed from the values in Table 2. Fig. 8 shows the normalized unit side resistance versus depth ratio. These figures show that, for D/B > 100 or so, micropiles and drilled shafts are approximately the same, although this pattern is not as clear as for cohesive soils. However, at shallower depths, there is an apparent increase for micropiles over larger-diameter drilled shafts, by typical factors in the range of 1.5 to 2.5 with values as high as 6. No

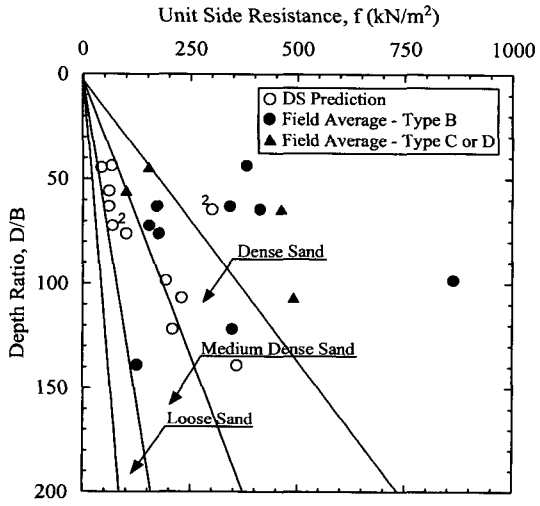

Fig. 7. Comparison of unit side resistance in cohesionless soils predicted by drilled shaft (DS) calculations and back-calculated field averages

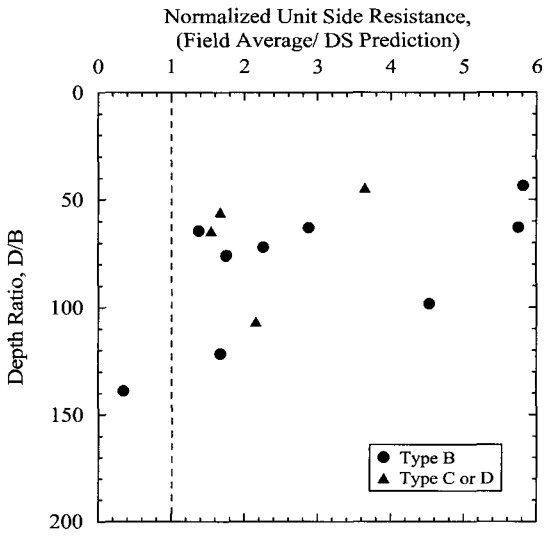

Fig. 8. Normalized unit side resistance in cohesionless soils vs. depth ratio

Table 2. Typical values of effective stress friction angle ($\overline{\phi}$) and overconsolidation ratio (OCR)

Soil Type	$\overline{\phi}$ (deg)	OCR
Loose Sand	28 ~32	1~3
Medium Dense Sand	32~83	3~10
Dense Sand	38~45	10~20

differentiation by micropile type is evident. Again, this increase results from the grouting during installation.

5. Summary

A database is developed with case histories of micropiles from ten sites with twenty-one axial compression load test results. The database is used to examine the load-displacement behavior as well as to estimate the axial compression capacity.

The initial slope of the load-displacement curve associated with high depth ratio for micropiles is less than the elastic slope. Therefore, the initial slope can be estimated by elastic slope for micropiles subjected to axial compression loading.

There is a significant difference in load-carrying capacity between micropiles and drilled shafts that results primarily from the micropile pressure-grouting installation effects on the state of stress in the ground. An increase in "effective diameter" also is likely for micropiles, but this effect could not be evaluated from the data. The results show that micropiles can have a significant increase of capacity over larger-diameter drilled shafts at shallower depths with D/B < 100 or so. In cohesive soils, the typical increase is on the order of 1.5 with values as high as 2.5. For cohesionless soils, the typical increases are in the range of 1.5 to 2.5 with values as high as 6. No micropile type difference is evident. At greater depths with D/B > 100 or so, micropiles and drilled shafts appear to have similar capacity.

The factors noted above should be investigated carefully when extrapolating design values from larger-diameter drilled shafts into micropile design practice. These values will need to be re-evaluated and refined as more and better quality data become available.

References

1. Bruce, D. A. (1987), "Rehabilitation of Main Repair Facility, Coney Island", *Preliminary Report*, Nicholson Construction, Pittsburgh.
2. Bruce, D. A. (1988), "Aspects of Minipiling Practice in the US", *Ground Engineering*, Vol.21, No.8, pp.20-33.
3. Bruce, D. A. (1989), "Aspects of Minipiling Practice in the US", *Ground Engineering*, Vol.22, No.1, pp.35-39.
4. Bruce, D. A. (1990), "Pin Pile Performance: Post Grouted Piles at Augusta", *GA. Technical Note B-5022*, Nicholson Construction,

Pittsburgh.

5. Bruce, D. A. and Juran, I. (1997), "Drilled and Grouted Micropiles: State-of-Practice Review", FHWA-RD-96-016, McLean, July.
6. Bruce, D. A. and Yeung, C. K.A (1984), "Review of Minipiling, with Particular Regard to Hong Kong Applications", *J. Hong Kong Institution of Engineers*, pp.31-54.
7. Bruce, D. A., Hall, C. H. and Triplett, R. E. (1992), "Structural Underpinning by Pinpiles", *Proceedings of the 17th Deep Foundations Institute Annual Meeting*, New Orleans, pp.49-78.
8. Bruce, D. A., Ingle, J. D. and Jones, M. R. (1985), "Recent Examples of Underpinning Using Mini- piles", *Proceedings of the 2nd International Conference on Structural Faults and Repairs*, London, pp.13-28.
9. Chen, J.-R. (1998), "Case History Evaluation of Axial Behavior of Augered-Cast-In-Place Piles and Pressure-Injected Footing", MS Thesis, Cornell University, Ithaca.
10. Chen, Y.-J. and Kulhawy, F. H. (1994), "Case History Evaluation of Behavior of Drilled Shafts Under Axial & Lateral Loading", *Report TR-104601*, Electric Power Research Institute, Palo Alto.
11. Davisson, M. T. (1972), "High Capacity Piles. Proceedings of Lecture Series on Innovations in Foundation Construction", *ASCE Illinois Section*, Chicago.
12. Hirany, A. and Kulhawy, F. H. (1988), "Conduct and Interpretation of Load Tests on Drilled Shaft Foundations: Detailed Guidelines", *Report EL-5915 (1)*, EPRI, Palo Alto.
13. Hirany, A. and Kulhawy, F. H. (1989), "Interpretation of Load Tests on Drilled Shafts-Part 1: Axial Compression", *Foundation Engineering*: Current Principles & Practices (GSP 22), Ed. FH Kulhawy, ASCE, New York, pp.1132-1149.
14. Ichimura, Y. and Oshita, T. (2000), "Applicability of Statnamic Load Test for Micropile", *Proceedings of the 3rd International Workshop on Micropiles*, Ube, Japan.
15. Jeon, S. S. (2004), "Interpretation of Load Test on Minipiles", *Proceedings of the Institution of Civil Engineers-Geotechnical Engineering*, Vol.157, No.2, pp.85-90.
16. Jones, D. A. and Turner, M. J. (1980), "Load Tests on Post-grouted Micropiles in London Clay", *Ground Engineering*, Vol.13, No.6, pp.47-53.
17. Koreck, H. W. (1978), "Small Diameter Bored Injection Piles", *Ground Engineering*, Vol.11, No.4, pp.14-29.
18. Kulhawy, F. H. (1991), *Drilled Shaft Foundations*. Chap. 14 in Foundation Eng. Handbook (2/E), Ed. H.-Y. Fang, Van Nostrand Reinhold, New York, pp.537-552.
19. Kulhawy, F. H. and Mayne, P. W. (1990), "Manual on Estimating Soil Properties for Foundation Design", *Report EL-6800*, EPRI, Palo Alto.
20. Lizzi, F. (1982) Static Restoration of Monuments, Sagep Publishers, Genoa.
21. Singh, S. and Heine, E. I. (1984), Upgrading Existing Footings with Micro-Piles. Proceedings of International Conference on Case Histories in Geotechnical Eng (3), St. Louis, pp.1373-1383.

(received on Mar. 2, 2004, accepted on Jul. 20, 2004)